Core of ^{25}F in the rotational model

A. O. Macchiavelli ⬤, R. M. Clark, H. L. Crawford, P. Fallon, I. Y. Lee ⬤, C. Morse, C. M. Campbell,
M. Cromaz, and C. Santamaria ⬤

Nuclear Science Division, Lawrence Berkeley National Laboratory, Berkeley, California 94720, USA

In a recent experiment, carried out at the Radioactive Isotope Beam Factory/RIKEN, the ^{25}F$(p, 2p)$ ^{24}O reaction was studied at 270 MeV/A in inverse kinematics. Derived spectroscopic factors suggest that the effective core of ^{25}F significantly differs from a free ^{24}O nucleus. We interpret these results within the particle-rotor model and show that the experimental level scheme of ^{25}F can be understood in the rotation-aligned coupling scheme with its $5/2_1^+$ ground state as the bandhead of a decoupled band. The excitation energies of the observed $1/2_1^+$ and $9/2_1^+$ states correlate strongly with the rotational energy of the effective core, seen by the odd proton, and allow us to estimate its 2^+ energy at ≈ 3.2 MeV and a moderate quadrupole deformation $\epsilon_2 \approx 0.15$. The measured fragmentation of the $\pi d_{5/2}$ single-particle strength is discussed, and some further experiments suggested.

Introduction. The structure of neutron-rich nuclei is a central theme of study in the field of nuclear structure. Of particular interest is the quest to understand the evolution of shell structure and collectivity with isospin. The emergence of the islands of inversion at $N = 8$, 20, and 40 are prime examples of such evolution and have provided strong evidence regarding the important role played by the neutron-proton interaction [1–6].

Another intriguing and dramatic impact of the action of the neutron-proton force is seen in the so-called oxygen neutron-dripline anomaly, at $N = 16$, which is extended to $N = 22$ in the F isotopes with just the addition of one $d_{5/2}$ proton. In a recent work [7], the structure of ^{25}F has been investigated via $(p, 2p)$ quasifree knockout experiments with exclusive measurements using a ^{25}F beam at the Radioactive Isotope Beam Factory/RIKEN. The analysis of measured cross sections and derived spectroscopic factors may imply that the effective core of ^{25}F consists of a mixture of approximately 35% of ^{24}O in its ground state (gs) and 65% in excited configurations. As discussed by the authors, their results suggest that the addition of the $0d_{5/2}$ proton considerably changes the neutron structure in ^{25}F from that in ^{24}O and calls for a revision to the np tensor interaction in the widely used effective interactions, which appears to be too weak to reproduce the observations. In contrast, studies of neutron decay from unbound excited states in ^{24}O [8] and one-neutron removal from ^{24}O [9] were indicative of a $N = 16$ shell closure and the doubly magic nature of this nucleus. The relatively high excitation energy $E_x = 4.7 \pm 0.1$ MeV and the small $B(E2) \approx 0.5$ WU (Weisskopf units) of the 2_1^+ state [10] has further supported this interpretation.

In this Rapid Communication, we follow up on our earlier work [11] and interpret the above results in terms of a collective picture within the framework of the particle-rotor model (PRM) [12,13] to provide further insight into the nature of the effective ^{24}O core in ^{25}F.

The Structure of ^{25}F. The structure of odd-A nuclei usually offers fingerprints that can disentangle the competition of single-particle and collective effects if these degrees of freedom can be described, at least *a priori*, in terms of a nucleon coupled to a core. Considering ^{24}O as our core, an inspection of the Nilsson diagram [14] in Fig. 1 suggests that the odd proton will occupy the single-j multiplet originating from the $d_{5/2}$ orbit, namely, the levels $[220]\frac{1}{2}$, $[211]\frac{3}{2}$, and $[202]\frac{5}{2}$ with its Fermi energy at the $[220]\frac{1}{2}$ level, indicated by the wavy line in Fig. 1.

The effects of rotation on the single-particle motion are well understood, and the PRM has been very successful in explaining the observed near-*yrast* structures in deformed nuclei [15].

The PRM Hamiltonian can be written as [12,13]

$$H = H_p + \frac{\hbar^2}{2\mathscr{I}}\vec{R}^2, \tag{1}$$

where H_p is the Nilsson Hamiltonian [14] for the particle in the absence of rotation, $\mathscr{I}$ and $\vec{R}$ are the moment of inertia and the angular momentum of the core, respectively. Replacing $\vec{R} = \vec{I} - \vec{j}$ in Eq. (1) gives the usual expression,

$$H = E_\Omega + \frac{\hbar^2}{2\mathscr{I}}I(I + 1) + H_c, \tag{2}$$

where E_Ω's are the intrinsic level energies and H_c is the Coriolis coupling term,

$$H_c = -\frac{\hbar^2}{2\mathscr{I}}(I_+ j_- + I_- j_+), \tag{3}$$

where $I_\pm$ and $j_\pm$ are the ladder operators for the total and single-particle angular momenta, respectively. This coupling is particularly important for small deformations and large j values, and increases with the rotational frequency ω_{rot}. The Coriolis K mixing gives rise to a wave function of the general
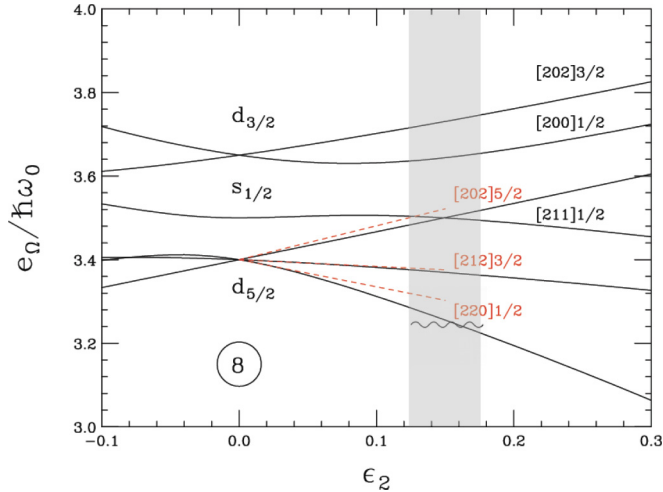
FIG. 1. Nilsson levels relevant for the structure of positive-parity proton states in ^{25}F with the red dashed lines representing the single-j approximation of the $d_{5/2}$ multiplet. The shaded area indicates the anticipated ϵ_2 deformation, and the wavy line indicates the Fermi level of the odd proton. Energies are in units of the harmonic-oscillator frequency $\hbar\omega_0$.

form

$$\psi_I = \sum_K \mathcal{A}_K |\, IK \rangle. \qquad (4)$$

The ratio of the Coriolis matrix elements in Eq. (3) ($H_c \sim \hbar^2 Ij/\mathscr{I} \sim j\hbar\omega_{\rm rot}$) to the intrinsic level spacings ($\Delta E \sim \epsilon_2\hbar\omega_0$) serves as a control parameter defining the characteristics of the coupling between collective and intrinsic angular momenta. For $H_c/\Delta E \ll 1$, the particle remains strongly coupled to the core maintaining the projection of its angular momentum on the symmetry axis Ω as a good quantum number. When $H_c/\Delta E \gg 1$, a rotation-aligned coupling limit is anticipated [15,16]. In this case, the *yrast* band has spins $I = j,\ j + 2,\ j + 4, \ldots$, and the energy spacings equal that of the core; this type of band is referred to as a decoupled band. The two limiting cases are illustrated in Fig. 2.

Results: Level energies. The experimental level scheme of ^{25}F [17], shown in Fig. 3(a), exhibits an interesting pattern having the first two *yrast* states with spins $5/2_1^+$ and $9/2_1^+$ and a conspicuous $1/2_1^+$ state in between. In analogy with our interpretation in Ref. [11] of the structure of ^{29}F [18], the *yrast* states can be associated with members of the decoupled band based on the $d_{5/2}$ multiplet for which we have $(j\omega_{\rm rot})/(\epsilon_2\omega_0) > 1$. The $1/2_1^+$ must have antiparallel coupling of $\vec{j}$ with the core rotation $\vec{R}$. It follows that, in the decoupled limit ($\epsilon_2 \to 0$), the energy of the $1/2_1^+$ state with respect to the ground state is proportional to the rotational energy of the core $E_{2^+}(\text{core})$. Together with the $9/2_1^+$ state, they provide a proxy for the 2^+ energy of the effective ^{24}O core in ^{25}F. Adjusting to the energies of the $1/2_1^+$ and $9/2_1^+$ states gives $E_{2^+}(core) \approx 3.2$ MeV, in line with a modest quadrupole deformation $\epsilon_2 \approx 0.15$, and consistent with the conditions required for the appearance of a decoupled band.

The results obtained of the PRM calculations, shown also in Fig. 3(b) are in good agreement with the experimental data
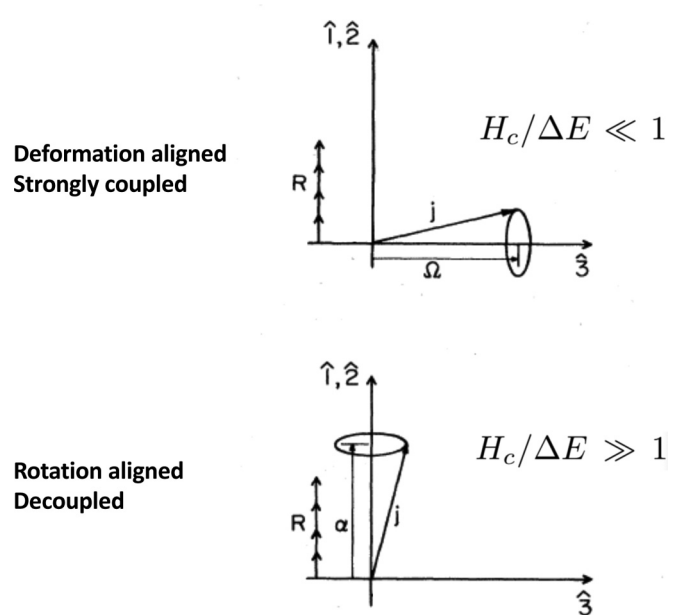

FIG. 2. Schematic of the strongly coupled and decoupled limits of the PRM. The latter is used, here, in our description of ^{25}F. The symmetry axis is labeled $\hat{3}$. Collective rotation takes place around a perpendicular axis ($\hat{1}, \hat{2}$). The figure is adapted from Ref. [15].

and give support to the rotational model description. Furthermore, in the rotation-aligned coupling limit the amplitudes $\mathcal{A}_K$ entering in Eq. (4) are given by the Wigner $\mathbb{d}$ function evaluated at $\pi/2$, the angle between the symmetry ($\hat{3}$) and rotation axes ($\hat{1}, \hat{2}$,) [15],

$$\mathcal{A}_K \approx \mathbb{d}_{5/2,K}^{5/2}(\pi/2). \qquad (5)$$

In ^{26}F [19], the 1^+ ground and 4^+ isomeric states can be associated with the antiparallel and parallel couplings of the odd neutron in the $d_{3/2}$ Nilsson multiplet to the structure of ^{25}F. The former, favored by the Gallagher-Moszkowski rule [20], gives 1^+ as the lowest state and the latter as 4^+ as the bandhead of a doubly decoupled band.

Spectroscopic factors. We now proceed with the calculation of spectroscopic factors for the $(-1p)$ knockout reaction and compare them to those reported in Ref. [7]. Following the formalism discussed in Ref. [21], which we recently applied to a similar case in ^{18,19}F [22], we obtain the expression,

$$S_{i,f}(j\ell) = \left(\sum_K \mathcal{A}_K \theta_{i,f}(j\ell, K) \right)^2, \qquad (6)$$

$$\theta_{i,f}(j\ell, K) = \sqrt{2}\langle I_i jK\Omega_\pi | I_f 0 \rangle C_{j,\ell} \langle \phi_f | \phi_i \rangle \qquad (7)$$

where $\mathcal{A}_K$ are given in Eq. (5), $\langle | \rangle$ is a Clebsch-Gordan coefficient and $\langle \phi_f | \phi_i \rangle$ represents the core overlap between the initial and the final states, typically assumed to be 1. Since we are considering a single-j approximation for the $d_{5/2}$ Nilsson multiplet, the amplitudes $C_{j,\ell}$ are equal to 1. Special care should be taken to assure consistency between the relative phases of the $\mathcal{A}_K$ Coriolis-mixed amplitudes and the Clebsch-Gordan coefficients entering in the sum.

In Table I, the spectroscopic factors are compared to the measurement reported in Ref. [7]. The PRM is able to explain
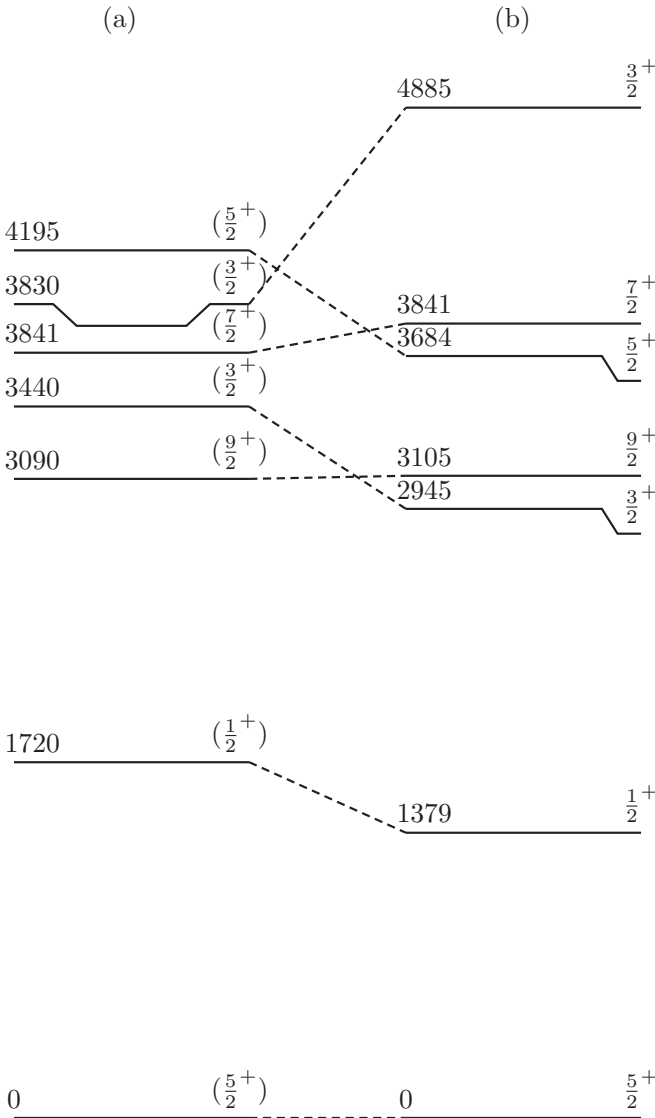
FIG. 3. (a) The experimental level scheme of ^{25}F from Ref. [17]. (b) Results of the PRM calculations. Energies are in keV.

the level scheme of ^{25}F but predicts a small fragmentation of the $d_{5/2}$ proton strength with $\approx 15\%$ going to the 2^+ and 4^+ of ^{24}O (PRM1). However, the premise of a substantial difference between the initial and the final cores requires that the overlap in Eq. (7) should be considered explicitly. We use the

TABLE I. Comparison of the measured spectroscopic factors to the PRM results, with (PRM1) and without core overlap (PRM2). Also shown are shell-model calculations using the SDPF-MU interaction.

Final state in ^{24}O	$S_{\exp}$ Ref. [7]	S_{th} PRM1	PRM2	SDPF-MU
Ground	0.36(13)	0.85	0.56	0.95
Excited	0.65(25)	0.15	0.44	0.05

TABLE II. Electromagnetic properties of the low-lying levels of ^{25}F in the PRM. Magnetic moments have been calculated using $g_R = Z/A$ and $g_s = 0.7(g_s)_{\text{free}}$.

I^{π}	E_x (MeV)	μ (μ_N)	Q ($e\text{fm}^2$)	$B(E2; I \to \frac{5}{2}^+)$ (WU)
$\frac{5}{2}^+$	0	3.9	-4.5	
$\frac{1}{2}^+$	1.4	1.9	0	3.9
$\frac{9}{2}^+$	3.1	4.6	-7.8	1.9

method described in Refs. [23,24] and obtain[1] $\langle \phi_f | \phi_i \rangle \approx 0.81$ bringing the PRM result closer to the observations (PRM2).

For reference, we also include the shell-model results using the SDPF-MU interaction given in Ref. [7]. Note, if the authors of Ref. [7] had corrected the gs to gs spectroscopic factor by a quenching factor of ≈ 0.6, usually observed in $(p, 2p)$ reactions [25], the agreement would have been excellent.

Obviously, additional studies of proton addition and removal reactions will be of interest, specifically proton knockout or $(d, {}^3\text{He})$ from ^{26}Ne come to mind. Here, anticipating that $\langle \phi_f | \phi_i \rangle \sim 1$, we predict a spectroscopic factor for the 0^+ to $5/2^+$ transition $S_{if} \approx 1.25$.

Conclusion. The rotational model is able to describe the structure of ^{25}F as arising from the coupling of a proton $d_{5/2}$ Nilsson multiplet to an effective core of modest deformation $\epsilon_2 \approx 0.15$. These conditions anticipate that the development of a decoupled band should be favorable and, indeed, PRM calculations show that the rotation-aligned coupling scheme is in agreement with the observed levels. Using the formalism developed for studies of single-nucleon transfer reactions in deformed nuclei, we calculated the proton spectroscopic factors for the ^{25}F$(5/2^+)(-1p)^{24}$O reaction. Agreement with the experimental data [7] is obtained by the fragmentation of the $d_{5/2}$ strength due to both deformation and a core overlap.

The Nilsson plus PRM picture suggests that the extra proton with a dominant component in the down-sloping $[220]\frac{1}{2}$ level polarizes ^{24}O and stabilizes its dynamic deformation. Thus, the effective core in ^{25}F can be interpreted as a slightly deformed rotor with $E_{2^+}(\text{core}) \approx 3.2$ MeV and $\epsilon_2 \approx 0.15$, compared to the real doubly magic ^{24}O with $E_{2^+} \approx 4.7$ MeV and weak vibrational quadrupole collectivity.

Furthermore, electromagnetic observables for the three lowest experimental levels obtained in the PRM (Table II), suggest that measurements of the magnetic and quadrupole moments of the $5/2^+$ state as well as a Coulomb excitation measurement of the transition probabilities will definitely shed further light on the validity of our interpretation.

---

[1]A simple volume overlap gives $\langle \phi_f | \phi_i \rangle \approx \frac{1}{1 + \epsilon_2 + \frac{2}{3}\epsilon_2^2 + \cdots} \approx 0.85$.

[1] T. Otsuka, A. Gade, O. Sorlin, T. Suzuki, and Y. Utsuno, Rev. Mod. Phys. **92**, 015002 (2020), and references therein.

[2] O. Sorlin and M. Porquet, Prog. Part. Nucl. Phys. **61**, 602 (2008).

[3] A. Poves and J. Retamosa, Phys. Lett. B **184**, 311 (1987).

[4] T. Otsuka, R. Fujimoto, Y. Utsuno, B. A. Brown, M. Honma, and T. Mizusaki, Phys. Rev. Lett. **87**, 082502 (2001).

[5] K. Heyde and J. L. Wood, Rev. Mod. Phys. **83**, 1467 (2011).

[6] E. K. Warburton, J. A. Becker, and B. A. Brown, Phys. Rev. C **41**, 1147 (1990).

[7] T. L. Tang *et al.*, Phys. Rev. Lett. **124**, 212502 (2020).

[8] C. R. Hoffman *et al.*, Phys. Lett. B **672**, 17 (2009).

[9] R. Kanungo *et al.*, Phys. Rev. Lett. **102**, 152501 (2009).

[10] K. Tshoo *et al.*, Phys. Rev. Lett. **109**, 022501 (2012).

[11] A. O. Macchiavelli *et al.*, Phys. Lett. B **775**, 160 (2017).

[12] S. G. Nilsson and I. Ragnarsson, *Shapes and Shells in Nuclear Structure* (Cambridge University Press, Cambridge, UK, 1995).

[13] S. E. Larsson, G. Leander, and I. Ragnarsson, Nucl. Phys. A **307**, 189 (1978).

[14] S. G. Nilsson, Mat. Fys. Medd. Dan. Vid. Selsk. **29**, No. 16, 1 (1955).

[15] F. S. Stephens, Rev. Mod. Phys. **47**, 43 (1975).

[16] F. S. Stephens, R. M. Diamond, and S. G. Nilsson, Phys. Lett. B **44**, 429 (1973).

[17] Zs. Vajta *et al.*, Phys. Rev. C **89**, 054323 (2014).

[18] P. Doornenbal *et al.*, Phys. Rev. C **95**, 041301(R) (2017).

[19] A. Lepailleur *et al.*, Phys. Rev. Lett. **110**, 082502 (2013).

[20] C. G. Gallagher and S. A. Moszkowski, Phys. Rev. **111**, 1282 (1958).

[21] B. Elbek and P. O. Tjøm, in *Advances in Nuclear Physics*, edited by M. Baranger and E. Vogt (Springer, Boston, MA, 1969), pp. 259–323.

[22] A. O. Macchiavelli, H. L. Crawford, P. Fallon, I. Y. Lee, R. M. Clark, C. M. Campbell, M. Cromaz, C. Morse, and C. Santamaria, Phys. Rev. C **101**, 044319 (2020).

[23] T. Takemasa, M. Sakagami, and M. Sano, Phys. Rev. Lett. **29**, 133 (1979).

[24] T. Takemasa, Comput. Phys. Commun. **36**, 79 (1985).

[25] L. Atar *et al.*, Phys. Rev. Lett. **120**, 052501 (2018).